3D1-1

Classification of Terrain Using the Correlation Coefficient in the Circular Polarization Basis for X-band POLSAR data

Yukari Yamamoto[1], #Yoshio Yamaguchi1[1], Hiroyoshi Yamada[1], Ryoichi Sato[2], Jian Yang[3]
[1] Department of Information Engineering, Niigata University
Ikarashi 2-8050, Niigata, 950-2181, Japan, yamaguch@ie.niigata-u.ac.jp
[2] Department of Education, Niigata University
[2] Department of Electronics, Tsinghua University

1. Introduction

Classification of terrain is one of the most important applications of Polarimetric Synthetic Aperture Radar (POLSAR) sensing. This paper presents a simple method to classify terrain by the correlation coefficients in the circular polarization basis and the total power of scattering matrix in the X-band. It is known that the circular polarization correlation coefficient contains essential polarimetric indexes and plays the best performance in classification and detection of targets among various polarization bases. A slight modification of the correlation coefficient taking into account of reflection symmetry condition enables us to detect forest area and man-made targets effectively. A combination of the coefficient, its modification, and the total power information, leads us to classify terrain very effectively. This paper presents classified results using the X-band Pi-SAR dataset and comparison with photo ground truth data.

2. Correlation Coefficient in the Circular Polarization Basis

It has been known from experimental observations that the correlation coefficient in the circular polarization basis (LR) contains a lot of information with respect to physical correspondence such as 1) topology mapping [1], man-made target detection [2], [3], vegetation detection [4] in the L-band. We applied the correlation coefficient to extract forest area region in complex urban scenarios using X-band high resolution (1.5 by 1.5 m) and fully polarimetric Pi-SAR data.

The correlation coefficient in the circular polarization basis can be written in terms of scattering matrix elements as

$$\gamma_{LL-RR} = \frac{\left\langle 4 \left| S_{HV} \right|^2 - \left| S_{HH} - S_{VV} \right|^2 \right\rangle - j\, 4\,\mathrm{Re}\left\langle S_{HV}^{*} \left(S_{HH} - S_{VV} \right) \right\rangle}{\sqrt{\left\langle \left| S_{HH} - S_{VV} + j\,2S_{HV} \right|^2 \right\rangle \left\langle \left| S_{HH} - S_{VV} - j\,2S_{HV} \right|^2 \right\rangle}} \qquad (1)$$

The symbol $\langle \bullet \rangle$ denotes ensemble average. It has been known from experimental observations that the cross correlations between S_{HH} and S_{HV} or S_{VV} and S_{HV} become zero, i.e., $\langle S_{HH} S_{HV}^{*} \rangle \approx \langle S_{VV} S_{HV}^{*} \rangle \approx 0$ for natural distributed targets such as vegetations. This is called the reflection symmetry. Under the reflection symmetry condition, (1) reduces to the following form

$$\gamma_{LL-RR}(0) = \frac{\left\langle 4 \left| S_{HV} \right|^2 - \left| S_{HH} - S_{VV} \right|^2 \right\rangle}{\left\langle 4 \left| S_{HV} \right|^2 + \left| S_{HH} - S_{VV} \right|^2 \right\rangle}. \qquad (2)$$

This equation shows that the correlation coefficient becomes real number. If we plot the value in the complex plane, it locates in between 0 and -1 on the negative real axis since $\left\langle 4 \left| S_{HV} \right|^2 \right\rangle < \left\langle \left| S_{HH} - S_{VV} \right|^2 \right\rangle$ is usually satisfied for natural distributed area.

ISBN: 978-4-88552-223-9 C3055©IEICE

3. Pi-SAR Data Analysis

The area under study is Western Niigata area over which air-borne "Pi-SAR" took flight 4 times during 2004. The Pi-SAR has acquired scattering matrices both in the X-band and L-band. The resolution in the X-band is 1.5 by 1.5 m. The area includes sea, seashore, pine trees, crop fields, buildings, residential houses, rice paddy fields, and so on. Therefore the area consists of reflection symmetry targets as well as non-reflection symmetry targets. We applied the correlation coefficient to the datasets. Figure 1 shows the X-band total power image.

3.1 Distribution of the Correlation Coefficient

Some patch areas are specifically chosen for viewing the correlation coefficient distribution. The correlation coefficients in each patch are plotted in the complex plane in Fig.2.

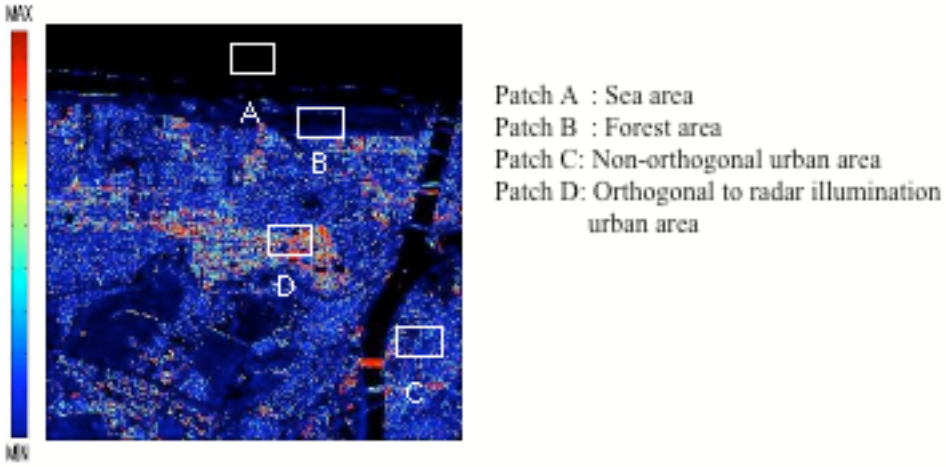

Fig. 1 X-band Pi-SAR total power image and patches for specific targets

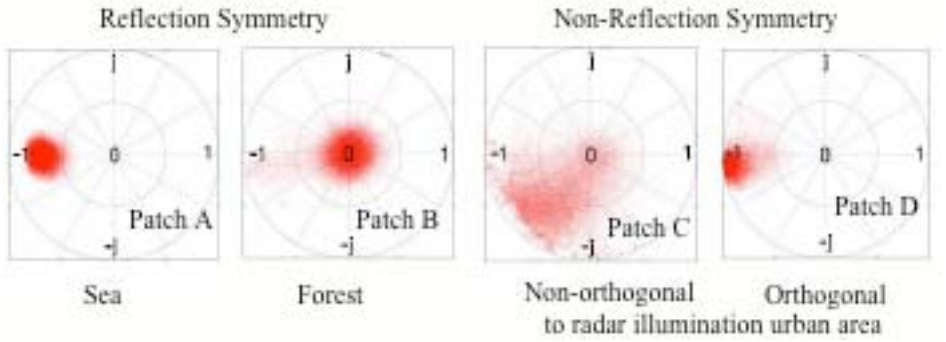

Fig.2 The distribution of the correlation coefficient in each patch.

It can be seen in Fig.2 that the distribution of reflection symmetry target (Patch A and B) locates around the negative axis and that the distribution of urban areas (mostly residential houses non-orthogonal to radar illumination) is spread. It is also interesting to note the distribution of forest (pine trees in this case) is localized around 0. In a similar manner, we have calculated out forest distributions for other areas. Comparing these distributions, we found out that the smaller magnitude of the correlation coefficient less than 0.3 corresponded to mainly forested area and to flat surface area such as road, ground, and water surface.

3.2 Detection of Forest Area

If we pay our attention to detect forested area, we need to specify the following condition:

$$|\gamma_{LL-RR}| < 0.3 \qquad (3)$$

And then in order to exclude the contribution from flat surface area, we use the value of total power. That is the radar cross section of target that is an essential parameter for any radar system. Through empirical condition, the exclusion criteria is set as

$$\text{Total power} < -13 \text{ dB} \qquad (4)$$

Using these two conditions (3) and (4), the forested area (tree area) detected in this Pi-SAR data became as shown in Fig.3, where $\frac{1}{|\gamma_{LL-RR}|}$ is displayed for illustration.

Fig.4 shows an aerial photo the corresponding region for validation purpose. If we compare bright (pine tree) area with aerial photo in Fig.4, perfect match can be observed. In addition, several bright spots in the middle of the image are recognized as trees by the eye inspection of Fig.4. Therefore one can easily recognize the tree area by this simple method.

Fig.3 Forest area extracted by the correlation coefficient and total power < -13 dB.

Fig.4 Aerial photo of Western Niigata area

3.3 Detection of non-orthogonal Urban Area

Since urban areas with non-orthogonal to radar illumination exhibit wide spread distribution (Fig.2), this information can be utilized to pick-up these areas. If we take the next index, the value should be close to unity for the reflection symmetry, and will diverse from unity for non-symmetric target.

$$\gamma'_{LL-RR} = \frac{|\gamma_{LL-RR}|}{\gamma_{LL-RR}(0)} \qquad (5)$$

We employed this idea for detection of non-orthogonal urban area. The typical values for specific regions are listed in Table 1. It is seen that the non-orthogonal urban areas have larger value compared to other areas.

Table 1. Typical value of γ'_{LL-RR}

Sea: 1.01	Sea-shore: 1.10	Forest: 1.44
Paddy rice field: 1.11	Crop field: 1.22	
Orthogonal urban area: 1.12	Non-orthogonal urban area: 2.54	

4. Classification Result

Finally, the polarimetric indexes on the total power of the scattering matrix, the correlation coefficient, and its modifications are combined to classify terrain observed by Pi-SAR system. Fig.5 shows the final classification result which is in good agreement with the ground truth data.

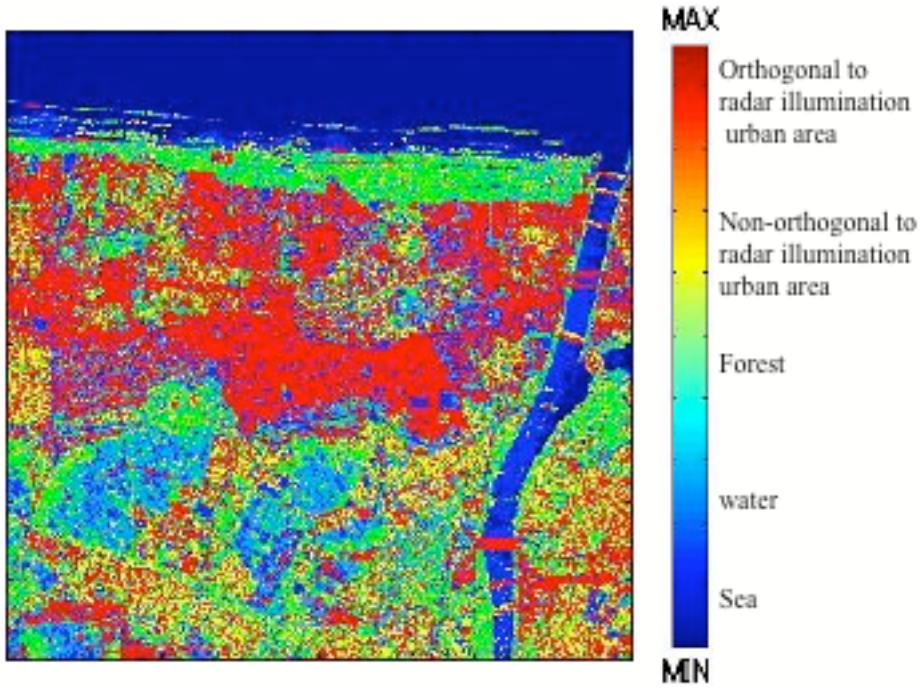

Fig.5 Color-coded classified image of the X-band Pi-SAR data.
(Western Niigata, Japan, data-take: 2004.8)

5. Conclusion

A combination of the coefficient, its modification, and the total power information, enables us to classify terrain very effectively. The classified results are illustrated using the X-band Pi-SAR dataset and compared with photo ground truth data. This simple method based on the polarimetric information serves well for accurate terrain classification.

Acknowledgments

The authors are grateful to NiCT and JAXA for providing Pi-SAR datasets. This work in part has been carried out by Grant-in-Aid for Scientific Research, JSPS, Japan.

References

[1] J. S. Lee, D. Schuler, T. L. Ainsworth, E. Krogager, D. Kasilingam, and W. M. Boerner, “On the estimation of radar polarization orientation shifts induced by terrain slopes,” *IEEE Trans. Geosci. Remote Sensing*, vol. 40, no. 1, pp. 30–41, Jan. 2002.

[2] K. Kimura, Y. Yamaguchi, H. Yamada, "Circular polarization correlation coefficient for detection of non-natural targets aligned not parallel to SAR flight path in the X-band POLSAR image analysis," *IEICE Trans. Commun.*, vol.E87-B, no.10, pp.3050-3056, Oct. 2004.

[3] T. Moriyama, Y. Yamaguchi, S. Uratsuka, T. Umehara, H. Maeno, M. Satake, A. Nadai, K. Nakamura, "A study on polarimetric correlation coefficient for feature extraction of polarimetric SAR data," *IEICE Trans. Commun.*, vol.E88-6, no.6, pp.235-2361, 2005.

[4] M. Murase, Y. Yamaguchi, and H. Yamada, "Polarimetric correlation coefficient applied to tree classification," *IEICE Trans. Commun.*, vol. E84-B, no. 12, pp. 1835-1840, Dec. 2001.